ISBN: 978-3-95450-249-3 ISSN: 2673-5350 doi: 10.18429/JACoW-IBIC2024-TUP68

DIAGNOSTICS BEAMLINE FOR THE SUPERCONDUCTING RF PHOTOINJECTOR TEST STAND AT DESY*

S. Jaster-Merz†, D. Bazyl, W. Decking, K. Floettmann, M. Krasilnikov, D. Lipka, S. Mogk, A. Novokshonov, E. Vogel, Deutsches Elektronen-Synchrotron DESY, Germany

Abstract

For future continuous wave (CW) and high-duty-cycle operation of the European XFEL, research and development of the DESY L-band CW photoinjector is ongoing. The implementation of a superconducting radio frequency (SRF) gun operated at 1.3 GHz with a copper photocathode is the baseline option. The electron beam quality, in particular the slice emittance, produced by this injector is key for the successful operation of the free-electron laser. In order to study the beam quality and stability of operation, a dedicated test stand and diagnostics beamline is being developed at DESY. Here, we present an overview of the foreseen diagnostic components and methods at the SRF CW photoinjector test stand.

INTRODUCTION

A future upgrade of the European XFEL to continuous wave (CW) and high-duty-cycle (HDC) operation is being explored to enable high average brilliance and a flexible time structure of the produced photon pulses for the users [1–3]. Such an upgrade requires a CW photoinjector capable of delivering electron bunches with a high electron quality, i.e., a small normalized emittance at the level of 0.2 µm for 100 pC charge bunches. A photoinjector based on the DESY CW L-band SRF gun cavity is the preferred solution. This design allows for high field gradients, high peak currents, and small transverse emittances and thus enables the direct matching of the beam into a booster cavity [4, 5]. The DESY CW SRF gun cavity with an integrated Cu cathode has repeatedly demonstrated a peak electric field on axis of up to 55 MV m^{-1} in vertical tests [5]. In order to characterize the electron beam quality produced by these SRF gun cavities, a dedicated SRF photoinjector test stand (Ts4i) [6] is being built at DESY. This includes a diagnostics beamline allowing for measurements of the energy, charge, emittances, and other beam parameters. Here, we present an overview of this Ts4i diagnostics beamline with a main focus on the foreseen diagnostic components and methods.

SRF PHOTOINJECTOR TEST STAND - TS4I

The SRF photoinjector test stand is designed and optimized for the electron bunch parameters expected from the DESY CW L-band SRF gun cavity. Bunches with 100 pC charge, an energy of 4 MeV to 6 MeV, and normalized transverse emittances from 0.2 µm to 0.4 µm are expected. A full list of the beam parameters is provided in Table 1. The Ts4i beamline consists of a cryostat hosting the SRF gun cavity, a superconducting (SC) solenoid for emittance compensation [7, 8], and two dipole steerers. The SC solenoid was produced by the company Niowave and is an improved copy of the model developed at HZB [9]. A commercial Pharos laser (PH1-20-0200-10-N2-NS) is foreseen to be installed on the roof of the Ts4i bunker. The wavelength of the laser beam will be converted from infrared to ultraviolet and is coupled into the beamline downstream of the cryostat. The complete layout of the test stand is shown in Fig. 1. The diagnostics beamline starting downstream of the cryostat consists of a straight and a dispersive section. Its main purpose is to characterize the quality and stability of the produced electron bunches as well as study the level of the dark current. A small transverse emittance is key for the successful operation of free-electron lasers (FELs) which require a high electron brightness. Especially the value of the transverse slice emittance is of interest as the performance of the FEL depends on the transverse emittance within one cooperation length [10, 11]. The diagnostics beamline is therefore specifically designed to measure the slice emittance of the beam.

Table 1: Design Beam Parameters

Parameter	Unit	Value
Beam energy	MeV	4 – 6
Charge per bunch	pC	100
Normalized emittance	µm	0.2 – 0.4
Repetition rate of bunches	MHz	0.1 – 1
Average beam current	µA	10 – 100

The different elements of the diagnostics beamline foreseen to perform all the above-mentioned measurements are described in more detail in the following while a more detailed description of the slice emittance measurement setup is provided in the next section.

Screen Stations

Four screen stations (S1 - S4) will be installed in the Ts4i diagnostics beamline to measure the transverse profiles of the bunches. When inserted into the beam path, the bunch repetition rate will be reduced to 10 Hz in order to protect the hardware components. All stations are European XFEL-type screen stations [12] with a 200 µm thick Gadolinium Aluminum Gallium Garnet doped with cerium (GAGG:Ce) scintillating screen [13]. The setup uses a 1:2 optics with a 45° observation angle and a Scheimpflug optics to reduce

* This work is performed in the framework of R&D for future accelerator operation modes at the European XFEL and is financed by the European XFEL GmbH.
† sonja.jaster-merz@desy.de

ISBN: 978-3-95450-249-3 ISSN: 2673-5350 doi: 10.18429/JACoW-IBIC2024-TUP68

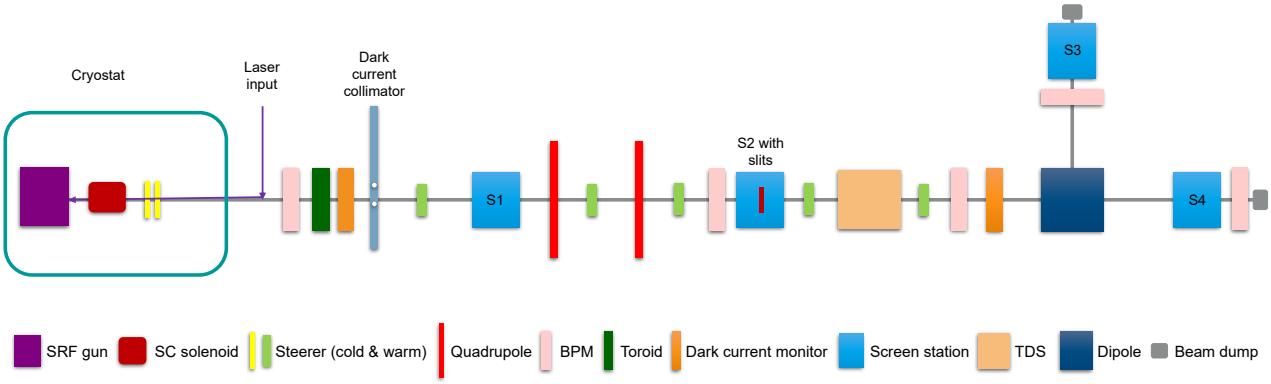

Figure 1: Schematic layout of the Ts4i beamline (not to scale).

the depth-of-field effect. The field of view is 16.90 mm × 14.14 mm with a nominal resolution of 30 µm × 8 µm.

In addition, the first screen station includes a scintillating screen with an increased thickness to measure the intensity and profile of the beam halo.

To measure the horizontal and vertical emittances, one horizontal and one vertical mover with one slit mask each is installed in the screen station S2. The slit masks are foreseen to be fabricated of Tantalum and have a slit width of 20 µm and a thickness of 0.5 mm. Simulations with the software G4BEAMLINE [14] showed that this slit mask configuration provides a sufficient signal-to-noise ratio with an expected value between 1×10^3 and 1×10^4 for the central beamlet. Space for an optional second slit mask on the horizontal mover is foreseen, thereby allowing for a choice between different slit widths based on the beam parameters. A rotational alignment of the slit mask can be performed remotely.

To resolve small features of the beam, the screen station S4 will house an additional setup that comprises the same scintillating screen material and thickness but a different optics setup thereby allowing for a better transverse resolution of approximately 3.5 µm × 3.5 µm [15].

Charge Measurement

The charge of the bunches can be measured by either using a toroid or a dark current monitor. Both devices are installed in series in the beamline to allow for cross-calibration. The dark current monitor is constructed such that it resonantly superimposes the dark current signal at the RF frequency of 1.3 GHz and thereby produces a sufficiently strong signal to measure the dark current. Additionally, the bunch charge can be measured on a second channel. A second dark current monitor is planned to be installed downstream of the slit mask to measure the charge of the beamlets with high precision down to ≤ 10 fC [16, 17].

Beam Position Monitors

Five beam position monitors (BPMs) of European XFEL type [18] using the FLASH electronics design [19] without a delay line are foreseen along the beamline to provide non-invasive beam trajectory measurements. After calibration with the other charge measurement devices, the BPMs can also be used to observe the charge transmission. Furthermore, the two BPMs at the end of the beamlines are used to monitor the safe dumping of the beam.

Transverse Deflection Structure

One transverse deflection structure (TDS) will be installed in the beamline to characterize the longitudinal properties of the bunch and enable slice emittance, bunch duration, current profile, and longitudinal phase space measurements. The foreseen TDS is operated at a frequency of 1.3 GHz at a 10 Hz repetition rate with a maximum streaking voltage of approximately 230 kV resulting in an achievable longitudinal resolution of 300 fs. Its design is identical to the TDS installed at HZB and is described in detail in [20].

Magnets

The beamline contains five dual-plane steerers [21] for the correction or the beam trajectory. Their locations are chosen such that the beam can be aligned to all magnets and screen stations as well as the TDS.

Two quadrupoles are foreseen upstream of the TDS to optimize the longitudinal resolution for slice emittance and longitudinal phase space measurements. The quadrupoles have an effective length of 40 mm and an expected field gradient of up to 5.7 T m^{-1}.

One spectrometer dipole will be installed to measure the energy and energy spread. The dipole deflects the beam by 90° onto the screen S3 with a horizontal offset of 0.88 m. To ease the beam setup for the best energy resolution, the screen station S4 in the straight section is placed at the same beam path distance to the dipole as the screen station S3. This allows for a minimization of the beta function at the screen S4 before performing the energy spread measurement on the dispersive screen S3.

ISBN: 978-3-95450-249-3 ISSN: 2673-5350 doi: 10.18429/JACoW-IBIC2024-TUP68

Dark current collimator

To reduce the amount of transported dark current, a collimator with hole apertures of various sizes will be installed similar to the device currently successfully in operation at the European XFEL [22]. These apertures can be moved into the beam path and aligned horizontally using actuators.

SLICE EMITTANCE MEASUREMENT

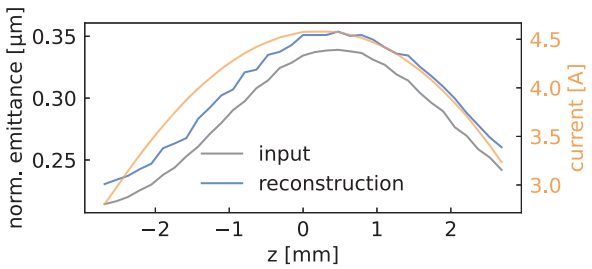

Figure 2: Reconstructed (blue) and input (gray) normalized slice emittance. Additionally, the input current profile is shown in orange color.

As previously noted, the slice emittance is an important parameter for FEL operation. The diagnostics beamline is therefore specifically designed to measure the horizontal slice emittance. This is done by combining a slit scan in the horizontal direction with the streaking of the beam in the vertical direction using a TDS.

The working principle of an emittance measurement based on the slit scan method is described in detail in, e.g., [23, 24]. To measure the emittance, a slit is moved through the beam path to cut out beamlets from the bunch which then propagate to a downstream screen. From the measured beamlet pattern at the screen, the beam matrix elements and hence the emittance can be reconstructed. The RMS spot size $\langle x^2 \rangle$ can be obtained from the slit positions x_i and the intensities I_i of the beamlets, where the index i refers to the i^{th} slit position. The RMS divergence $\langle x'^2 \rangle$ is calculated from the local angular deviation of the beamlets $x'_i = (X_i - x_i)/L$ and the RMS spread of the beamlets at the slit $\sigma_{x'_i} = \sigma_{X_i}/L$, where L is the drift length from the slit to the measurement screen, X_i are the mean beamlet position at the screen, and σ_{X_i} are the RMS spreads of the distribution at the screen. The correlation term $\langle xx' \rangle$ is obtained from the slit positions x_i and angular deviations x'_i of the beamlet, where both x_i and x'_i denote the deviations from the centroids of the distribution:

$$\begin{aligned} \langle x^2 \rangle &= \frac{\sum_i I_i x_i^2}{\sum_i I_i}, \\ \langle x'^2 \rangle &= \frac{\sum_i I_i (x_i'^2 + \sigma_{x'_i}^2)}{\sum_i I_i}, \\ \langle xx' \rangle &= \frac{\sum_i I_i x_i x'_i}{\sum_i I_i}. \end{aligned} \tag{1}$$

The emittance can then be calculated from these beam matrix elements using $\epsilon_x = \sqrt{\langle x^2 \rangle \langle x'^2 \rangle - \langle xx' \rangle^2}$. This slit-based method has the advantage over other emittance measurement schemes, such as magnet scans [25–27] or multi-screen approaches, that it converts a space-charge-dominated beam into the emittance-dominated regime, thereby improving the accuracy of the measurement [24].

To obtain time-resolved information about the bunches, a TDS can be used. A TDS imprints a longitudinally dependent transverse kick onto the bunch. The longitudinal profile is thereby mapped onto this transverse plane and can be measured at a downstream screen. The screen coordinate Δy can be converted into the longitudinal bunch coordinate Δz by using the shear parameter $S \approx \Delta y / \Delta z$ [28]. The shear parameter is given by [28] $S = 2\pi e f V M_{1,2}/(c^2 p)$, where p is the average momentum of the bunch, e the elementary charge, f the TDS working frequency, V the peak voltage, c the speed of light in vacuum, and the matrix element $M_{1,2} = L$ for a drift L between the TDS center and the screen. The achievable longitudinal resolution is given by $R = \sigma_y^{\text{off}}/S$, which is optimal for a phase advance of 90° between the TDS and screen. In case of a pure drift, the optimal resolution can be achieved by minimizing the unstreaked RMS spot size σ_y^{off} at the screen. By combining this vertical streaking of the bunch with a horizontal slit scan, the horizontal slice emittance can be measured.

Simulations of Slice Emittance Measurements

To verify the setup for the slice emittance measurements, simulation studies with two million particles using ASTRA [29] were performed. The solenoid and quadrupole strengths were optimized using the Python library optimas [30] to obtain a minimum transverse emittance at the slit location as well as the best possible longitudinal resolution for the TDS measurement. A radial uniform and longitudinal Gaussian laser pulse was assumed as this is the expected setup for the initial Ts4i operation. The gun gradient was set to a conservative estimate of 40 MV m^{-1}. The optimization result yielded a projected normalized horizontal emittance of 0.34 µm at the slit location. A longitudinal resolution of 530 fs was achieved and a 0.33 µm normalized horizontal emittance of the central slice. For the simulated emittance measurement, the 20 µm wide and 0.5 mm thick slit was moved through the beam in 50 µm steps covering a transverse range of $\pm 3\sigma$ of the horizontal RMS spot size. Space charge effects were included in the simulation. The reconstructed slice emittance and the original slice emittance of the distribution at the slit are shown in Fig. 2 together with the input current profile. The reconstructed slice emittance shows excellent agreement with the original distribution with a relative discrepancy below 5 % for the central slice. As the transverse emittance is reconstructed at the slit location and the longitudinal information is obtained at the TDS center, a possible bunch lengthening between these two locations is investigated in simulations. No significant differences between the current profiles and RMS bunch durations at the two locations are visible. The discrepancies are at least three orders of magnitude below the target resolution thereby indicating that no

ISBN: 978-3-95450-249-3 ISSN: 2673-5350 doi: 10.18429/JACoW-IBIC2024-TUP68

errors are expected due to the 43 cm drift between the two elements.

To test the feasibility of the setup also for other expected emittance values, the simulation of the slice emittance measurement was repeated for beams with a 0.2 µm to 0.4 µm normalized emittance in 0.1 µm steps. The particle distributions feature the same Courant-Snyder parameters as the optimized and start-to-end simulated case but have a different transverse emittance. As the unstreaked spot size at the screen is directly linked to the emittance, the longitudinal resolution of the measurement is different for each slice emittance measurement simulation. In a final experiment, this resolution would be optimized for each measurement separately. All horizontal projected and central slice emittances are reconstructed with an accuracy of $\leq 10\,\%$ demonstrating that the setup is suited for the slice emittance measurement of beams with the envisaged parameters.

No asymmetries between the two transverse planes are expected and therefore no direct measurement of the vertical slice emittance is foreseen. The measurement of the projected vertical emittance and thereby a comparison to the horizontal one will, however, be possible with the vertically movable slit mask installed also at the screen station S2.

CONCLUSION

A dedicated test stand to characterize the electron bunch quality produced by a 1.3 GHz SRF gun-based photoinjector is being built at DESY. The test stand includes a diagnostics beamline designed to validate the achievable beam parameters required for the operation of free-electron lasers. The presented beamline will allow for the characterization of the produced dark current and enable measurements of the charge and energy of the electron bunches, as well as of their longitudinal phase space and both transverse emittances. Particular emphasis is put on the measurement of the horizontal slice emittance. Simulation studies show that the slice emittance can be accurately reconstructed within 10 % for all expected emittance values. The impact of misalignments and jitters on the reconstruction is planned to be investigated in a future study. Detailed start-to-end simulations that verify the applicability of such an SRF gun-based photoinjector at the European XFEL show promising results [31] and are currently ongoing. The first beam operation is expected in 2027.

ACKNOWLEDGMENTS

We would like to thank all the technical groups at DESY involved in this project. Furthermore, we would like to thank H. Panuganti for information on the photocathode laser, Y. Chen for helpful discussions on photoinjectors, F. Mayet for advice on the screen station design, and H. Dinter for helpful discussions on steerer magnets and other beamline components. This work is performed in the framework of R&D for future accelerator operation modes at the European XFEL and is financed by the European XFEL GmbH. This research was supported in part through the Maxwell computational resources operated at Deutsches Elektronen-Synchrotron DESY, Hamburg, Germany. We acknowledge support from DESY (Hamburg, Germany and Zeuthen, Germany), a member of the Helmholtz Association HGF.

REFERENCES

[1] J. K. Sekutowicz *et al.*, "Feasibility of CW and LP Operation of the XFEL Linac", in *Proc. FEL'13*, New York, NY, USA, Aug. 2013, pp. 189–192. https://jacow.org/FEL2013/papers/TUOCNO04.pdf

[2] R. Brinkmann, E. Schneidmiller, J. K. Sekutowicz, and M. V. Yurkov, "Prospects for CW Operation of the European XFEL in Hard X-ray Regime", in *Proc. FEL'14*, Basel, Switzerland, Aug. 2014, pp. 210–214. https://jacow.org/FEL2014/papers/MOP067.pdf

[3] J. Sekutowicz *et al.*, "Research and development towards duty factor upgrade of the european x-ray free electron laser linac", *Phys. Rev. Spec. Top. Accel. Beams*, vol. 18, no. 5, p. 050 701, 2015. doi:10.1103/PhysRevSTAB.18.050701

[4] H. J. Qian and E. Vogel, "Overview of CW RF Guns for Short Wavelength FELs", in *Proc. FEL'19*, Hamburg, Germany, Aug. 2019, pp. 290–296. doi:10.18429/JACoW-FEL2019-WEA01

[5] E. Vogel *et al.*, "High gradients at SRF photoinjector cavities with low RRR copper cathode plug screwed to the cavity back wall", 2023. doi:10.48550/arxiv.org/abs/2310.02974

[6] TS4I, https://ts4i.desy.de/

[7] L. Serafini and J. B. Rosenzweig, "Envelope analysis of intense relativistic quasilaminar beams in rf photoinjectors: A theory of emittance compensation", *Phys. Rev. E*, vol. 55, no. 6, pp. 7565–7590, 1997. doi:10.1103/PhysRevE.55.7565

[8] K. Floettmann, "Emittance compensation in split photoinjectors", *Phys. Rev. Accel. Beams*, vol. 20, no. 1, p. 013 401, 2017. doi:10.1103/PhysRevAccelBeams.20.013401

[9] J. Völker *et al.*, "A Superconducting Magnetic Shield for the Photoelectron Injector of BERLinPro", in *Proc. SRF'19*, Dresden, Germany, Jun.-Jul. 2019, pp. 335–339. doi:10.18429/JACoW-SRF2019-MOP105

[10] F. Sannibale, "High-brightness electron injectors for high-duty cycle x-ray free electron lasers", *Front. Phys.*, vol. 11, 2023. doi:10.3389/fphy.2023.1187346

[11] C. Pellegrini, A. Marinelli, and S. Reiche, "The physics of x-ray free-electron lasers", *Rev. Mod. Phys.*, vol. 88, no. 1, p. 015 006, 2016. doi:10.1103/RevModPhys.88.015006

[12] C. Wiebers, M. Holz, G. Kube, D. Noelle, G. Priebe, and H.-C. Schroeder, "Scintillating Screen Monitors for Transverse Electron Beam Profile Diagnostics at the European XFEL", in *Proc. IBIC'13*, Oxford, UK, Sep. 2013, pp. 807–810. https://jacow.org/IBIC2013/papers/WEPF03.pdf

[13] A. I. Novokshonov *et al.*, "Scintillator Nonproportionality Studies at PITZ", in *Proc. IBIC'22*, Kraków, Poland, pp. 277–280, 2022. doi:10.18429/JACoW-IBIC2022-TUP21

ISBN: 978-3-95450-249-3 ISSN: 2673-5350 doi: 10.18429/JACoW-IBIC2024-TUP68

[14] T. J. Roberts, S. Ahmed, K. B. Beard, D. Huang, D. M. Kaplan, and L. K. Spentzouris, "G4Beamline Particle Tracking in Matter-dominated Beam Lines", in *Proc. EPAC'08*, Genoa, Italy, pp. 2776–2778, 2008. https://jacow.org/e08/papers/WEPP120.pdf

[15] F. Mayet, private communication, Jul. 2024.

[16] D. Lipka, J. Lund-Nielsen, and M. Seebach, "Resonator for Charge Measurement at REGAE", in *Proc. IBIC'13*, Oxford, UK, Sep. 2013, pp. 872–875. https://jacow.org/IBIC2013/papers/WEPF25.pdf

[17] T. Lensch, D. Lipka, R. Neumann, and M. Werner, "Comparison of Different Bunch Charge Monitors Used at the ARES Accelerator at DESY", in *Proc. IBIC'23*, Saskatoon, Canada, pp. 169–173, 2023. doi:10.18429/JACoW-IBIC2023-TU3I04

[18] D. Lipka, B. Lorbeer, D. Noelle, M. Siemens, and S. Vilcins, "Button BPM Development for the European XFEL", in *Proc. DIPAC'11*, Hamburg, Germany, May 2011, pp. 83–85. https://jacow.org/DIPAC2011/papers/MOPD19.pdf

[19] B. Lorbeer, N. Baboi, H. T. Duhme, and R. Neumann, "High Resolution and Low Charge Button and Strip-Line Beam Position Monitor Electronics Upgrade at Flash", in *Proc. IPAC'18*, Vancouver, Canada, Apr.-May 2018, pp. 1923–1926. doi:10.18429/JACoW-IPAC2018-WEPAF048

[20] G. Kourkafas, T. Kamps, A. Neumann, and B. Keune, "Transverse Deflecting Cavity for Longitudinal Beam Diagnostics at BERLinPro", in *Proc. LINAC'18*, Beijing, China, pp. 875–878, 2019. doi:10.18429/JACoW-LINAC2018-THPO083

[21] K. Flöttmann, "Design and Performance of Printed Circuit Steering Magnets for the FLASH Injector", in *Proc. IPAC'10*, Kyoto, Japan, May 2010, pp. 277–279. http://jacow.org/IPAC10/papers/MOPEB003.pdf

[22] S. Liu *et al.*, "Collimator Performance Study at the European XFEL", in *Proc. IPAC'19*, Melbourne, Australia, May 2019, pp. 1717–1720. doi:10.18429/JACoW-IPAC2019-TUPRB019

[23] M. Zhang, "Emittance formula for slits and pepper-pot measurement", Fermi National Accelerator Laboratory (FNAL), Batavia, IL, United States, Tech. Rep., 1996. https://lss.fnal.gov/archive/test-tm/1000/fermilab-tm-1988.pdf

[24] S. G. Anderson, J. B. Rosenzweig, G. P. LeSage, and J. K. Crane, "Space-charge effects in high brightness electron beam emittance measurements", *Phys. Rev. ST Accel. Beams*, vol. 5, no. 1, p. 014 201, 2002. doi:10.1103/PhysRevSTAB.5.014201

[25] J. Rees and L. Rivkin, "Measuring emittances and sigma matrices", Stanford Linear Accelerator Center (SLAC), CA, United States, Tech. Rep., 1984.

[26] M. Hachmann and K. Flöttmann, "Measurement of ultra low transverse emittance at regae", *Nucl. Instrum. Methods Phys. Res. A*, vol. 829, pp. 318–320, 2016. doi:10.1016/j.nima.2016.01.065

[27] M. G. Minty and F. Zimmermann, *Measurement and control of charged particle beams*. Springer Berlin Heidelberg, 2003. doi:10.1007/978-3-662-08581-3

[28] M. Röhrs, C. Gerth, H. Schlarb, B. Schmidt, and P. Schmüser, "Time-resolved electron beam phase space tomography at a soft x-ray free-electron laser", *Phys. Rev. Spec. Top. Accel. Beams*, vol. 12, no. 5, p. 050 704, 2009. doi:10.1103/PhysRevSTAB.12.050704

[29] K. Floettmann, "Astra: A space charge tracking algorithm", *Manual, Version 3.2*, 2017. https://www.desy.de/~mpyflo/Astra_manual/Astra-Manual_V3.2.pdf

[30] A. Ferran Pousa *et al.*, "Bayesian optimization of laser-plasma accelerators assisted by reduced physical models", *Phys. Rev. Accel. Beams*, vol. 26, no. 8, p. 084 601, 2023.

[31] D. Bazyl, Y. Chen, M. Dohlus, and T. Limberg, *Cw operation of the european xfel: Sc-gun injector optimization, s2e calculations and sase performance*, 2021. doi:10.48550/arxiv.org/abs/2111.01756